arXiv:0910.5235v3 [cond-mat.mes-hall] 3 Nov 2009

Molecular spintronics using noncollinear magnetic molecules

Alessandro Soncini* and Liviu F. Chibotaru
Institute for Nanoscale Physics and Chemistry (INPAC) and Division of Quantum and Physical Chemistry, Katholieke Universiteit Leuven, Celestijnenlaan 200F, B-3001 Heverlee, Belgium
(Dated: November 3, 2009)

We investigate the spin transport through strongly anisotropic noncollinear magnetic molecules and find that the *noncollinear magnetization* acts as a spin-switching device for the current. Moreover, spin currents are shown to offer a viable route to selectively prepare the molecular device in one of two degenerate noncollinear magnetic states. Spin-currents can be also used to create a non-zero density of toroidal magnetization in a recently characterized Dy_3 noncollinear magnet.

One of the most ambitious directions in the quest for the ultimate miniaturization of electronic devices is represented by molecular spintronics [1, 2]. Molecular nanomagnets are particularly promising for nanospintronics, especially in relation to the quest for magnetic molecular qubits [3], since transport experiments [4, 5, 6] have shown a strong interplay between the current and the magnetic states of the molecules. To date, all theoretical investigations on molecular spintronics have addressed systems whose magnetism is only weakly anisotropic, thus exploring systems whose magnetization aligns along a single anisotropy axis (collinear magnetism) [7, 8, 9, 10]. The noncollinear regime of molecular magnetism, arising when the on-site magnetic anisotropy of single metal ions is one of the dominant energy scales, has only been explored very recently [11]. In the noncollinear regime magnetic molecules can be prepared in degenerate states characterized by non-dipolar magnetic moments, such as the recently predicted [11] and found [12, 13] toroidal (or anapole) moment in molecular wheels.

There are two main arguments that make spintronics of noncollinear magnets of great interest. The first follows from studies on spin-transport through mesoscopic rings with noncollinear internal magnetic fields, which have been predicted to produce spin-switching effects [14]. The size of noncollinear molecular scatterers is expected to be more favorable to overcome dephasing, and lead to the observation of coherence and spin-switching effects. The second argument is related to the use of noncollinear states to implement molecular qubits. On the one hand, molecular spin-qubits can easily be addressed via a magnetic field [15], although intermolecular dipolar interactions lead to short dephasing times [16]. On the other hand, intermolecular interactions between non-dipolar states are weak [11], thus decoherence times longer, although these states cannot be addressed via uniform fields. Spintronics might offer a promising strategy to address noncollinear protected molecular qubits.

In this Letter we investigate spin transport through molecular noncollinear magnetic states, and provide evidence that these systems do offer strategies to (i) implement quantum-interference molecular devices capable of reversing the polarization of an injected spin-current, and to (ii) selectively populate specific noncollinear magnetic states. The most relevant transport regime has been shown to be the Coulomb blockade (CB) [6]. The lowest lying states of a nanomagnet with n unpaired electrons well localized on N metal centers with local spin s is well described by the Hamiltonian:

$$\mathrm{H}_n \;=\; -J\sum_{\langle ij\rangle}\tilde{\mathbf{s}}_i\cdot\tilde{\mathbf{s}}_j + D\sum_i \tilde{s}^2_{z,i} \qquad (1)$$

consisting of the isotropic Heisenberg exchange coupling between nearest neighbors with strength J, and easy-axis zero-field splitting (ZFS) on-site (strength D with $D<0$). Note that the spin operator $\tilde{\boldsymbol{s}}_i$ has z-component $\tilde{s}_{i,z}$ parallel to the local ZFS axis. Whereas previous investigations [10] only considered the collinear weak-anisotropy regime, here we introduce two key-ingredients for *noncollinearity* [11]: (i) $|D| >> |J|$ (ii) on-site easy-axes *not parallel* to each other. In this work we will explore spin-transport for a dimer (Fig. 1, top) and a three-centers molecular wheel (Fig. 1, bottom).

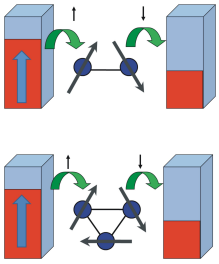

FIG. 1: (color online) The two molecular spintronics setups considered in this work. Top, a noncollinear antiferromagnetic dimer with on-site spin $s = 3/2$ and coplanar on-site ZFS easy-axes, tilted with respect to the perpendicular to the inter-metal distance by $\pm 30^\circ$. Bottom, a 3-center antiferromagnetic molecular wheel with on-site spin $s = 3/2$ and coplanar on-site ZFS easy-axes, arranged tangentially to the wheel's circumference (cf Ref. [11, 12]).

When connected to source, drain and gate electrodes, under bias voltage V_B and gate voltage V_G, the molecule will become charged. The migrating electron will be consecutively accommodated at different metal sites [17], described here by a set of N atomic orbitals localized on the metal centers. The molecular Hamiltonian for a charged

state with an excess of Q electrons with respect to the isolated nanomagnet is given by:

$$\begin{aligned} \mathrm{H}_{n+Q} &= \mathrm{H}_n + (\epsilon - eQV_G)\sum_{p}^{N}\sum_{\sigma}^{\uparrow\downarrow} n_{p\sigma} \\ &+ t\sum_{\langle pq\rangle}\sum_{\sigma}^{\uparrow\downarrow} c^{\dagger}_{p\sigma}c_{q\sigma} + U\sum_{p}^{N} n_{p\uparrow}n_{p\downarrow} \\ &+ J_{\mathrm{H}}\sum_{p}^{N}\sum_{\alpha}^{\uparrow\downarrow}\sum_{\beta}^{\uparrow\downarrow} \tilde{\boldsymbol{s}}_p \cdot \boldsymbol{\sigma}_{p,\alpha\beta} c^{\dagger}_{p\alpha}c_{p\beta}, \end{aligned} \qquad (2)$$

where ϵ is the energy of the localized orbitals, $c^{\dagger}_{p\sigma}$ are creation operators for the on-site spin-orbitals, $n_{p\sigma} = c^{\dagger}_{p\sigma}c_{p\sigma}$, t is a hopping parameter between centers, U is the Coulomb repulsion between two electrons on the same center, $\boldsymbol{\sigma}_p$ are Pauli matrices associated to an electronic spin injected on site p, and J_H is the Hund's rule coupling between the spin of the excess electron on site p, and the spin moment $\tilde{\boldsymbol{s}}_p$ on that center ($J_H < 0$). Here we confine ourselves with the region around the first CB diamond, where only singly-charged states are relevant together with the neutral ones. This is formally achieved by setting $U \to \infty$. Finally, a tunneling Hamiltonian $\mathrm{H}_{\mathrm{mix}}$ between electrodes and device is introduced in the usual manner [7, 8, 9, 10], with tunneling amplitudes estimated to be at most 0.3 cm^{-1} [6, 9]. Given the weak molecule-lead coupling, the transition rates W between molecule and contacts are calculated with the Fermi golden rule using $\mathrm{H}_{\mathrm{mix}}$, assuming a Fermi-Dirac distribution in the two leads, kept at different chemical potential $\mu_L - \mu_R = eV_B$. Next, using the rates W, a master equation for the non-equilibrium populations of charged and neutral states of the device is set up and solved in the steady-state regime. The resulting populations are used to compute the input $(I^{\uparrow}_L - I^{\downarrow}_L)$ and the output $(I^{\uparrow}_R - I^{\downarrow}_R)$ spin currents.

Let us first consider the dimer molecule with local spin $s = 3/2$ (*e.g.*, a Co(II) dimer). We assume co-planar local ZFS axes, forming angles $\theta = \pm 30°$ with the perpendicular (z-direction) to the Co-Co bond, (Fig. 1, top). We choose here $D = 5J$, with antiferromagnetic isotropic exchange coupling $J = -50$ cm^{-1}. The dominant energy scale in (2) is the on-site Hund coupling exchange J_H, chosen here as $J_H = 4D \approx 0.1eV$. Moreover, the source contact is assumed to be ferromagnetic, the drain non-magnetic. The spin-polarization axis for the ferromagnetic source is coplanar to the ZFS axes, and parallel to z (Fig. 1). The Heisenberg states of lower energy of the Co-dimer can be described in terms of almost pure noncollinear Ising states $|m_1 m_2\rangle$, where m_i is the projection of the local spin moment s along the tilted easy axis [11]. This is verified by decomposing the Heisenberg wavefunction into the noncollinear Ising basis. For the present choice of parameters, denoting "+" and "−" the on-site spin-states $|\pm 3/2\rangle$, the ground state is quasi-degenerate and corresponds to the in-phase and out-of-phase superposition of the noncollinear Neel states $|{+}{-}\rangle$, and $|{-}{+}\rangle$. The tunneling gap is about $\Delta \approx 0.38$ cm^{-1}.

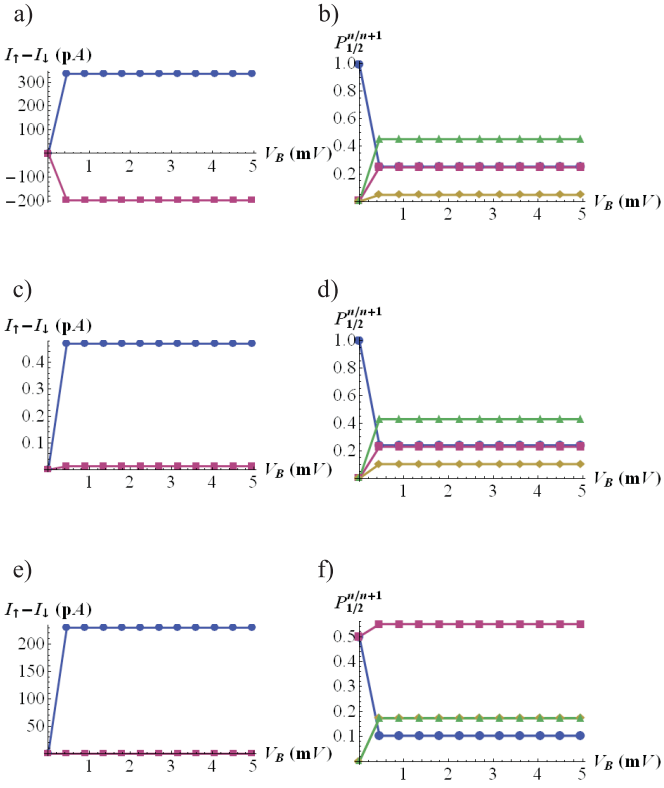

FIG. 2: (color online) Input (blue bullet datapoints) and output (purple square datapoints) spin-current vs. voltage curves (left column), and, (right column) non-equilibrium populations of neutral (blue bullet for in-phase and purple square for out-of-phase superposition of $|{+}{-}\rangle$ and $|{-}{+}\rangle$) and charged states (green upward-pointing triangles for $\Psi^{n+1}_{0,1}$, yellow diamonds for $\Psi^{n+1}_{0,2}$) for the noncollinear magnetic dimer, with the following type of exchange interaction and values of the transfer parameters ($D = -250$ cm^{-1}): a) and b) Heisenberg, $t = 0.5D$, c) and d) Heisenberg, $t = 4.0D$, e) and f) noncollinear Ising, $t = 1.0D$.

Next, we find the eigenstates of (2). We explore here two limiting situations: a weak-transfer limit with $t = 0.5D$, and a strong-transfer limit with $t = 4D = J_H$. In the weak-transfer limit, we expect the additional electron spin to follow "adiabatically" the noncollinear magnetic texture of the molecular device, so that the ground state of the charged system will be doubly degenerate, and dominated by either the $|{+}{-}\rangle$ or the $|{-}{+}\rangle$ component of the Neel doublet, carrying an additional electron on either center, with the spin parallel to the local magnetic moment via Hund-rule coupling. These expectations are confirmed by full diagonalization, leading to the following ground state for the $n+1$-magnet:

$$\begin{aligned} \Psi^{n+1}_{0,1} &\approx C_{\uparrow,0}\,|{+}{-}\rangle\,|\uparrow\,0\rangle + C_{0,\downarrow}\,|{+}{-}\rangle\,|0\,\downarrow\rangle \\ \Psi^{n+1}_{0,2} &\approx C_{\downarrow,0}\,|{-}{+}\rangle\,|\downarrow\,0\rangle + C_{0,\uparrow}\,|{-}{+}\rangle\,|0\,\uparrow\rangle\,, \end{aligned} \qquad (3)$$

where the kets $|\uparrow 0\rangle$ denote the determinant of two spin-orbitals centered on the two metals, the first with spin $\uparrow$, the second empty. We find $|C_{\uparrow,0}|^2 = |C_{\downarrow,0}|^2 \approx 0.45$, and $|C_{0,\downarrow}|^2 = |C_{0,\uparrow}|^2 \approx 0.42$. On the other hand, in the strong-transfer limit, inter-center hopping processes have the same rate as Hund-coupling spin-polarization processes, so that transport is not expected to be adiabatic. This is confirmed by full diagonalization, where the ground state is dominated by noncollinear Ising states favoring spin-preserving hopping processes, such as $|{+}{+}\rangle\,|\uparrow 0\rangle$ and $|{+}{+}\rangle\,|0\uparrow\rangle$. Thus, in this regime the overlap with the neutral noncollinear Neel states is very small. The voltage V_G is taken large enough to bring in resonance the ground states of the neutral and charged systems, separated by about $1eV$. Without loss of generality, we set the equilibrium chemical potential lying in between the ground and first excited state of the neutral molecule, and the temperature to $T = 0.1K$.

In Fig. 2a (weak-transfer) and 2c (strong-transfer) we report the spin current-voltage diagrams obtained for the two limits of the hopping parameter. Since the source is fully spin-polarized, the input spin current (blue bullets) always corresponds to the total charge-current. Interestingly, in the weak-transfer limit the output spin-current (purple square datapoints) has a negative sign: *the spin polarization of the input current is reversed in the output non-magnetic electrode, by the noncollinear magnetic texture*. On the other hand, in the strong-transfer regime this *spin-switching* effect is not observed. These results are easily interpreted analyzing the ground state wavefunctions for the neutral and charged states. In the weak-transfer limit, the charged ground state (3) is a coherent state describing the adiabatic hopping of an injected electron-spin between the two metals, in which process the additional electron always aligns its spin parallel to the magnetic polarization of the local metal ion. Thus we define this limit as the *adiabatic-transport limit*, in analogy with the findings reported in ref. [14] Although the CB-regime is non-coherent, the transition rates entering the master equation are determined by the overlap amplitudes between the tunneling combinations of the ground noncollinear Neel doublet, and the charged ground-state doublet (3). Due to the full $\uparrow$-spin polarization of the source, the injected electron on the first metal center creates an excess of non-equilibrium population in the state $\Psi_{0,1}^{n+1}$ (see Fig. 2b, green triangular datapoints), which can host an electron with spin-up on the first metal. The electron is then coherently transported through $\Psi_{0,1}^{n+1}$ on the second metal center, where, as described by the $|0\downarrow\rangle$ component of $\Psi_{0,1}^{n+1}$, its spin-polarization is reversed. Output tunneling events from the second metal center into the drain will thus occur more frequently with opposite spin-polarization. Since the additional spin-polarized electron collapses the tunneling wavefunction into one of the two Neel states, at non-zero bias voltage we note that the ground state and first excited tunneling states of the neutral system become equally populated (see Fig. 2b and 2d).

We note that the coupling between $|{+}{-}\rangle\,|\uparrow 0\rangle$ and $|{+}{-}\rangle\,|0\downarrow\rangle$ in (3), which determines the spin-switching transport, is triggered by the Hund-Hamiltonian. Importantly, if the angle θ is set to zero, *i.e.* within the collinear regime, the Hund-mechanisms leading to the superposition (3) are not active. Hence, *noncollinearity is found to be a crucial ingredient for the realization of the spin-switching effect*. In the non-adiabatic regime, the spin-switch effect is quenched (Fig. 2c) due to the negligible presence of spin-switch coherences in the charged ground state. In this limit the large hopping integral favors spin-preserving hopping processes. The current magnitude is also significantly smaller due to the small overlap between charged and neutral states (see Fig. 2c).

It is interesting to investigate the case of exact degeneracy between $|{+}{-}\rangle$ and $|{-}{+}\rangle$, implied by the noncollinear Ising exchange Hamiltonian:

$$\mathrm{H}_n \;=\; -J_I \sum_{\langle ij\rangle} \tilde{s}_{i,z}\tilde{s}_{j,z} + D\sum_i \tilde{s}_{z,i}^2. \qquad (4)$$

The ground state of the charged system for $t = D$ is still doubly degenerate and given by (3), with $|C_{\uparrow,0}|^2 = |C_{0,\downarrow}|^2 = |C_{\downarrow,0}|^2 = |C_{0,\uparrow}|^2 = 0.41$. The full $\uparrow$-spin polarization of the source electrode will favor population-transfer processes mainly between the $|{+}{-}\rangle$ Neel state and the *spin-switch* excited state $\Psi_{0,1}^{n+1}$, via the Hund-coupling mechanism. However, now only half of the input $\uparrow$-current is converted to $\downarrow$-current, so that the current is non-polarized in the drain (see Fig 2e). This can be rationalized in terms of additional population-transfer between $|{-}{+}\rangle$ and $\Psi_{0,2}^{n+1}$, since the latter contains 7% of the Hund-unstable component $|{-}{+}\rangle\,|\uparrow 0\rangle$. However, the dominant population-transfer process remains $|{+}{-}\rangle \rightarrow \Psi_{0,1}^{n+1}$, and, as seen from Fig. 2f, this fact has a fundamental consequence: *at non-zero bias voltage the spin-current causes a net excess of population of one of the two degenerate noncollinear Neel states*. Thus, the neutral system is prepared in the $|{-}{+}\rangle$ state.

Finally, we consider a 3-center molecular wheel with local ZFS axes contained in the molecular plane and tangential to the wheel's circumference. This system is of special interest, being a model for the experimentally characterized lanthanide wheel Dy_3 [18], which has been recently shown to have almost tangential on-site anisotropy axes, leading to toroidal magnetization [12]. For simplicity, here we consider an analog of this system with $s = 3/2$ on metal sites. The collective states are modelled by the noncollinear Ising Hamiltonian (4), with ferromagnetic exchange $J_I = 25\ \mathrm{cm}^{-1}$, and easy-axis ZFS parameter $D = 8J_I$. The ground state of the 3-wheel is a doubly degenerate Kramer's doublet characterized by a toroidal magnetic moment $\tau = \mu_B R \sum_p \tilde{s}_{z,p}$ [11, 12],

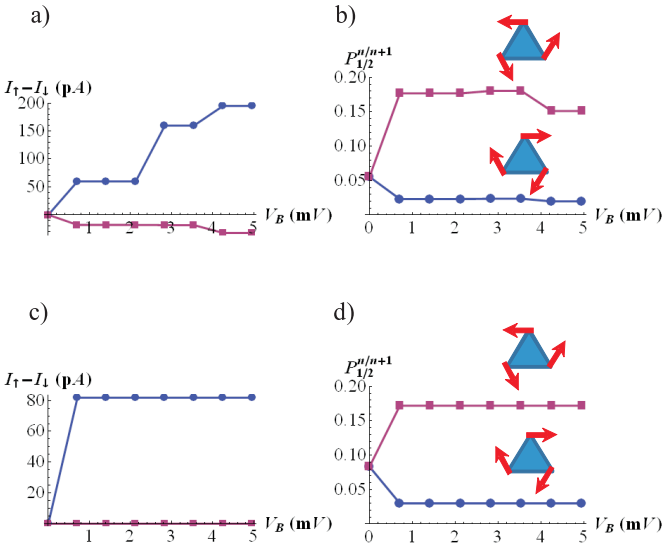

FIG. 3: (color online) Input (blue bullet datapoints) and output (purple square datapoints) spin-current vs. voltage curves (left column), and, (right column) non-equilibrium populations of neutral (blue bullet for $|---\rangle$ and purple square for $|+++\rangle$) for the 3-center noncollinear magnetic wheel, with the following values of the transfer parameters: a) and b) $t = 0.05D$, c) and d) $t = 1.0D$ ($D = -200$ cm^{-1}).

where R is the radius of the triangle, and μ_B is the Bohr magneton. We denote the two states with $|+++\rangle$ ($\tau = +9/2R\mu_B$) and $|---\rangle$ ($\tau = -9/2R\mu_B$), where the first position refers to the atom more strongly bound to the ferromagnetic source, and the second position refers to the atom bound to the non-magnetic drain. The singly-charged system is investigated for $J_H = 4D$, and for $t = 0.05D$ (adiabatic transfer) and $t = D$ (strong-transfer). The ground state of the singly charged system is always 4-fold degenerate. The present spintronics setup (bottom of Fig. 1, spin-polarization axis of the source co-planar with the wheel's plane, and perpendicular to the bond between metal 1 and metal 2) implies that only those components of the charged ground state overlapping with the $|---\rangle$ toroidal state reported in Fig. 1 will be significantly populated, by virtue of the Hund's coupling rule. In the adiabatic limit these states correspond to spin-switching states, *i.e.* to states which represent coherent hopping from center 1 to center 2, with inversion of spin-polarization, and found to be:

$$\begin{aligned}\Psi^{n+1}_{0,1} &\approx |---\rangle\,(a_1\,|\uparrow 00\rangle + b_1\,|0\downarrow 0\rangle)\\ \Psi^{n+1}_{0,2} &\approx |---\rangle\\ &\times\ (a_2\,|\uparrow 00\rangle + b_2\,|0\downarrow 0\rangle + c_2\,|00\uparrow\rangle + c_2\,|00\downarrow\rangle)\end{aligned}$$

with $|a_1|^2 = 0.4$, $|b_1|^2 = 0.38$, $|a_2|^2 = 0.21$, $|b_2|^2 = 0.27$, and $|c_2|^2 = 0.19$. In the non-adiabatic limit the weight of the spin-switching components becomes smaller (although does not vanish), in favor of states representing spin-conserving hopping processes.

In figure 3a (adiabatic) and 3c (nonadiabatic) we report the spin current-voltage diagrams obtained for the two limits of the hopping parameter: as for the dimer system, we observe spin switching only in the adiabatic limit. However, due to the spin-polarization of the source electrode, the population transfer from the $|---\rangle$ toroidal neutral state to the charged manifold always dominates the non-coherent kinetics, producing an excess of population of $|+++\rangle$, in both weak and strong transfer limits (Fig. 3b and 3d). This demonstrates a viable spintronics strategy to prepare a non-zero density of toroidal molecular magnetization in the sample.

In conclusion, we have investigated spin-transport through noncollinear magnetic molecules in the sequential tunneling (CB) regime. Two fundamental phenomena are identified here. The first, the *spin-switching effect*, is caused by the action of the noncollinear magnetization on the spin-current. The second, the *selective population bias* of one of the two partners of a noncollinear doublet, is determined by the effect of a spin-current on the noncollinear states. Non-collinearity is found to be the crucial ingredient in these phenomena. This work represents the first step into the new domain of noncollinear molecular spintronics, expected to have a significant impact on the quest for protected molecular qubits.

* Electronic address: Alessandro.Soncini@chem.kuleuven.be

[1] A. Rocha *et al.*, Nature Mater. **4**, 335 (2005);
[2] L. Bogani and W. Wernsdorfer, Nature Mater. **7**, 179 (2008).
[3] G. A. Timco *et al.*, Nature Nanotech. **4**, 173 (2009).
[4] J. Park *et al.*, Nature **417**, 722 (2002).
[5] W. Liang *et al.*, Nature **417**, 725 (2002).
[6] H. B. Heersche *et al.*, Phys. Rev. Lett. **96**, 206801 (2006); M-H. Jo *et al.*, NanoLett. **6**, 2014 (2006).
[7] F.Elste and C. Timm, Phys. Rev. B **71**, 155403 (2005).
[8] C. Romeike *et al.*, Phys. Rev. Lett. **96**, 196601 (2006).
[9] G. Gonzales and M.N. Leuenberger, Phys. Rev. Lett. **98**, 256804 (2007).
[10] M. Misiorny and J. Barnas, Phys. Status Solidi B **246**, 695 (2009).
[11] A. Soncini and L. F. Chibotaru, Phys. Rev. B **77**, 220406(R) (2008).
[12] L. F. Chibotaru, L. Ungur and A. Soncini, Angew. Chem. Int. Ed. **47**, 4126 (2008).
[13] J. Luzon *et al.*, Phys. Rev. Lett. **100**, 247205 (2008).
[14] D. Frustaglia, M. Hentschel and K. Richter, Phys. Rev. Lett. **87**, 256602 (2001).
[15] F. Troiani *et al.*, Phys. Rev. Lett. **94**, 207208 (2005).
[16] A. Morello *et al.*, Phys. Rev. Lett. **97**, 207206 (2006).
[17] L.F. Chibotaru *et al.*, J. Am. Chem. Soc. **125**, 12615 (2003).
[18] J. Tang *et al.*, Angew. Chem. Int. Ed. **45**, 1729 (2006).